

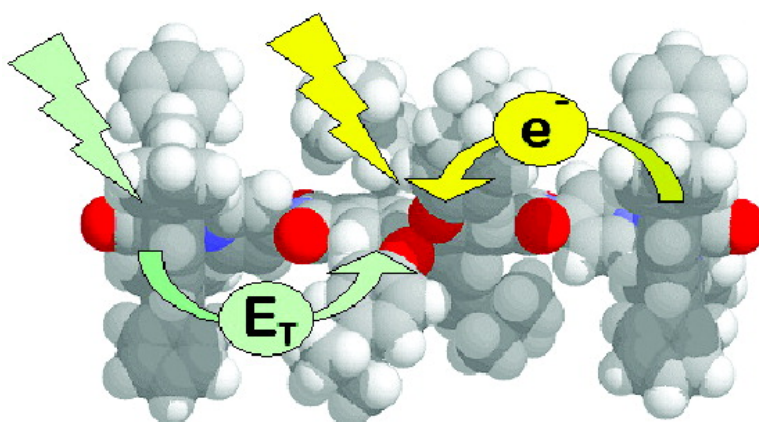
Article

Wavelength-Dependent Electron and Energy Transfer Pathways in a Side-to-Face Ruthenium Porphyrin/Perylene Bisimide Assembly

Anna Prodi, Claudio Chiorboli, Franco Scandola, Elisabetta Iengo, Enzo Alessio, Rainer Dobrawa, and Frank Wrthner

J. Am. Chem. Soc., **2005**, 127 (5), 1454-1462 • DOI: 10.1021/ja045379u • Publication Date (Web): 15 January 2005

Downloaded from <http://pubs.acs.org> on March 24, 2009



More About This Article

Additional resources and features associated with this article are available within the HTML version:

- Supporting Information
- Links to the 27 articles that cite this article, as of the time of this article download
- Access to high resolution figures
- Links to articles and content related to this article
- Copyright permission to reproduce figures and/or text from this article

[View the Full Text HTML](#)



ACS Publications
High quality. High impact.

Wavelength-Dependent Electron and Energy Transfer Pathways in a Side-to-Face Ruthenium Porphyrin/Perylene Bisimide Assembly

Anna Prodi,[†] Claudio Chiorboli,[‡] Franco Scandola,^{*,†,‡,§} Elisabetta Ingo,^{*,¶}
Enzo Alessio,[¶] Rainer Dobrawa,[#] and Frank Würthner^{*,#}

Contribution from the Dipartimento di Chimica, Università di Ferrara, 44100 Ferrara, Italy, ISOF-CNR, Sezione di Ferrara, 44100 Ferrara, Italy, INSTM, Sezione di Ferrara, 44100 Ferrara, Italy, Dipartimento di Scienze Chimiche, Università di Trieste, 34127 Trieste, Italy, and Institut für Organische Chemie, Universität Würzburg, 97074 Würzburg, Germany

Received July 31, 2004; E-mail: franco.scandola@unife.it

Abstract: A new side-to-face supramolecular array of chromophores, where a pyridyl-substituted perylene bisimide dye axially binds to two ruthenium porphyrin fragments, has been prepared by self-assembly. The array is formulated as DPyPBI[Ru(TPP)(CO)]₂, where DPyPBI = *N,N'*-di(4-pyridyl)-1,6,7,12-tetra(4-*tert*-butylphenoxy)perylene-3,4:9,10-tetracarboxylic acid bisimide and TPP = 5,10,15,20-tetraphenylporphyrin. The photophysical behavior of DPyPBI[Ru(TPP)(CO)]₂ has been studied by fast (nanoseconds) and ultrafast (femtoseconds) time-resolved techniques. The observed behavior sharply changes with excitation wavelength, depending on whether the DPyPBI or Ru(TPP)(CO) units are excited. After DPyPBI excitation, the strong fluorescence typical of this unit is completely quenched, and time-resolved spectroscopy reveals the occurrence of photoinduced electron transfer from the ruthenium porphyrin to the perylene bisimide dye ($\tau = 5.6$ ps) followed by charge recombination ($\tau = 270$ ps). Upon excitation of the Ru(TPP)(CO) fragments, on the other hand, ultrafast ($\tau < 1$ ps) intersystem crossing is followed by triplet energy transfer from the ruthenium porphyrin to the perylene bisimide dye ($\tau = 720$ ps). The perylene-based triplet state decays to the ground state on a longer time scale ($\tau = 9.8$ μ s). The photophysics of this supramolecular array provides remarkable examples of (i) wavelength-dependent behavior (a small change in excitation wavelength causes a sharp switch from electron to energy transfer) and (ii) intramolecular sensitization (the triplet state of the perylene bisimide, inaccessible in the free dye, is efficiently populated in the array).

Introduction

Because of their outstanding spectroscopic and photophysical properties, porphyrins and metalloporphyrins have been widely used in the construction of supramolecular arrays mimicking light-induced functions of natural photosynthesis.^{1,2} In most of such supramolecular arrays, the molecular components are connected by covalent linkages (usually through the meso positions of the porphyrin ring).³ Other synthetic approaches have also been successfully used, however, leading to various kinds of noncovalent multiporphyrin assemblies,⁴ such as hydrogen-bonded⁵ or metal-bridged⁶ assemblies.

We have been particularly interested in the implementation of a "side-to-face" assembling strategy, exploiting the coordination ability of peripheral pyridyl groups of one porphyrin toward the metal center of another porphyrin. The key to the stability

of axially ligated porphyrins is the strength of the coordinative bond between the side ligand and the metal ion of the face porphyrin(s). For example, ligation of pyridyl rings to zinc porphyrins is intrinsically weak (association constant, ca. 1×10^3 M⁻¹)⁷ and relatively labile; thus, in solution, coordination oligomers are generally in equilibrium with the monomers. The presence of monomers is of particular importance at the low

[†] Università di Ferrara.

[‡] ISOF-CNR.

[§] INSTM.

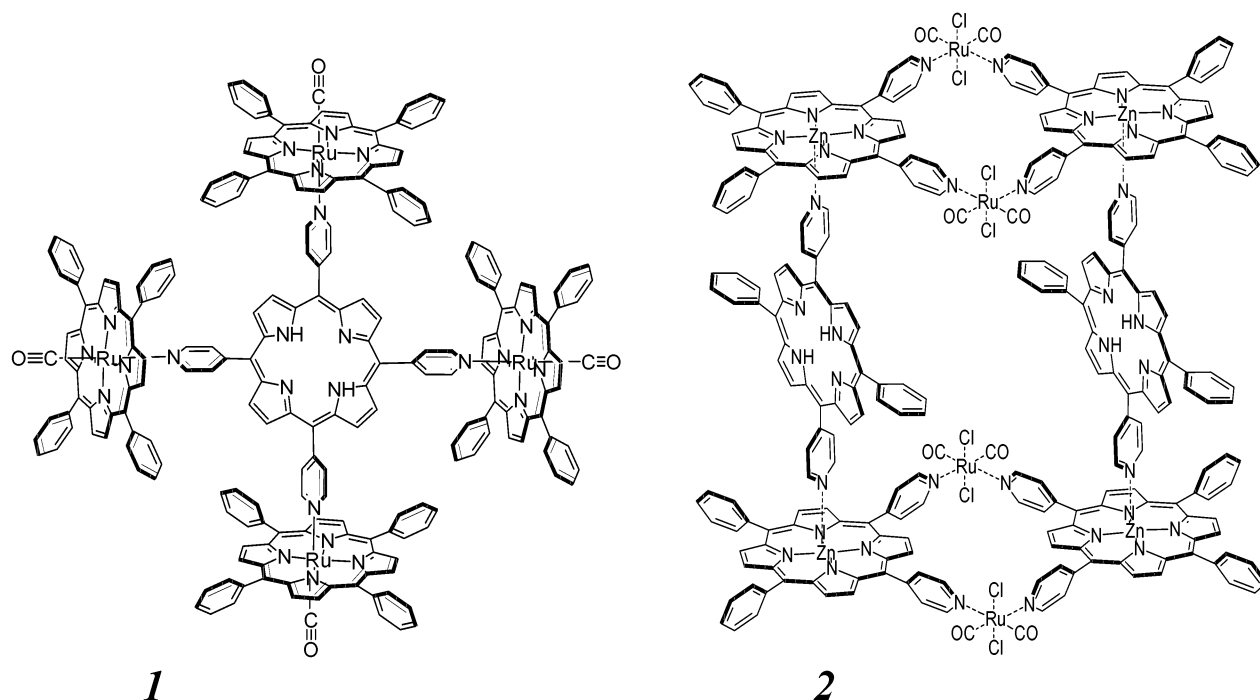
[¶] Università di Trieste.

[#] Universität Würzburg.

(1) Wasielewski, M. R. *Chem. Rev.* **1992**, *92*, 435–461. (b) Harriman, A.; Sauvage, J.-P. *Chem. Soc. Rev.* **1996**, 41–48. (c) Gust, D.; Moore, T. A.; Moore, A. L. *Acc. Chem. Res.* **1993**, *26*, 198–205. (d) Choi, M.-S.; Yamazaki, T.; Yamazaki, I.; Aida, T. *Angew. Chem., Int. Ed.* **2004**, *43*, 150–158.

(2) Anderson, S.; Anderson, H. L.; Bashall, A.; McPartlin, M.; Sanders, J. K. M. *Angew. Chem., Int. Ed. Engl.* **1995**, *34*, 1096–1200. (b) Davila, J.; Harriman, A.; Milgrom, L. R. *Chem. Phys. Lett.* **1987**, *136*, 427–430. (c) Prathapan, S.; Johnson, T. E.; Lindsey, J. S. *J. Am. Chem. Soc.* **1993**, *115*, 7519–7520. (d) Hsiao, J.-S.; Krueger, B. P.; Wagner, R. W.; Johnson, T. E.; Delaney, J. K.; Mauzerall, D. C.; Fleming, G. R.; Lindsey, J. S.; Bocian, D. F.; Donohoe, R. J. *J. Am. Chem. Soc.* **1996**, *118*, 11181–11193. (e) Nakano, A.; Osuka, A.; Yamazaki, I.; Yamazaki, T.; Nishimura, Y. *Angew. Chem., Int. Ed.* **1998**, *37*, 3023–3027. (f) Kuciauskas, D.; Liddell, P. A.; Lin, S.; Johnson, T. E.; Weghorn, S. J.; Lindsey, J. S.; Moore, A.; Moore, T. A.; Gust, D. *J. Am. Chem. Soc.* **1999**, *121*, 8604–8614. (g) Anderson, H. L. *Chem. Commun.* **1999**, 2323–1330. (h) Kim, Y. H.; Jeong, D. H.; Kim, D.; Jeong, S. C.; Cho, H. S.; Kim, S. K.; Aratani, N.; Osuka, A. *J. Am. Chem. Soc.* **2001**, *123*, 76–86. (i) Yang, S. I.; Prathapan, S.; Miller, M. A.; Seth, J.; Bocian, D. F.; Lindsey, J. S.; Holten, D. *J. Phys. Chem. B* **2001**, *105*, 8249–8258. (j) Taniguchi, M.; Ra, D.; Kirmaier, C.; Hindin, E. K.; Schwartz, J. K.; Diers, J. R.; Bocian, D. F.; Lindsey, J. S.; Knox, R. S.; Holten, D. *J. Am. Chem. Soc.* **2003**, *125*, 13461–13470. (k) Takahashi, R.; Kobuke, Y. *J. Am. Chem. Soc.* **2003**, *125*, 2372–2373. (l) Balaban, T. S.; Bhise, A. D.; Fischer, M.; Linke-Schaetzl, M.; Roussel, C.; Vanthuyne, N. *Angew. Chem., Int. Ed.* **2003**, *42*, 2140–2144. (m) Pen, X.; Aratani, T.; Matsumoto, T.; Kawai, T.; Hwang, I.-W.; Ahn, T. K.; Kim, D.; Osuka, A. *J. Am. Chem. Soc.* **2004**, *126*, 4468–4469.

Chart 1



concentrations used for photophysical measurements (ca. 1×10^{-6} M). More stable assemblies of well-defined stoichiometry require cooperative coordination or strict geometrical complementarity of the building blocks.⁸ Less labile metal ions, such as Ru(II), have been used to obtain kinetically inert and

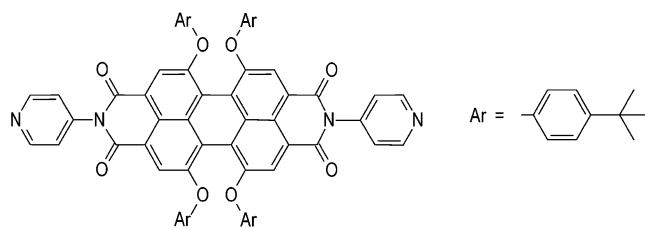
thermodynamically stable assemblies of side-to-face porphyrins⁹ and, more generally, architectures featuring facing porphyrin cores bridged by nitrogen ligands.¹⁰ Within this framework, we have reported two examples of side-to-face arrays obtained by Ru–pyridyl and Zn–pyridyl coordination, the pentameric (**1**)¹¹ and hexameric (**2**)^{8b} structures (Chart 1), both showing good stability in a wide range of concentrations (as low as 1×10^{-7} M). In such arrays, efficient energy transfer from the metal porphyrins to the free base pyridylporphyrin was observed, at the triplet level in **1**¹¹ and at the singlet level in **2**.¹²

Another class of attractive building blocks for photoactive supramolecular architectures is that of perylene bisimide (PBI) dyes.¹³ They are characterized by extremely efficient fluorescent emission, facile electrochemical reduction, and clear spectroscopic signatures in the radical anion form.¹⁴ For these useful features, PBI units have been included as photoexcitable and/or electron-acceptor molecular components in a variety of interesting photoactive supramolecular systems.¹⁵

- (3) Gust, D.; Moore, T. A.; Moore, A. L. In *Electron Transfer in Chemistry*; Balzani, V., Ed.; Wiley-VCH: Weinheim, Germany, 2001; Volume III, Part 2, Chapter 2, pp 273–336. (b) Burrell, A. K.; Officer, D. L.; Plieger, P. G.; Reid, D. C. W. *Chem. Rev.* **2001**, *101*, 2751–2796. (c) Aratani, N.; Osuka, A.; Cho, H. S.; Kim, D. *J. Photochem. Photobiol. C* **2002**, *3*, 25–52.
- (4) Chambron, J.-C.; Heitz, V.; Sauvage, J.-P. In *The Porphyrin Handbook*; Kadish, K.; Smith, K. M., Guillard, R., Eds.; Academic Press: San Diego, CA, 2000; Volume 6, pp 1–42. (b) Wojaczyński, J.; Latos-Grażyński, L. *Coord. Chem. Rev.* **2000**, *204*, 113–171. (c) Imamura, T.; Fukushima, K. *Coord. Chem. Rev.* **2000**, *198*, 133–156. (d) Iengo, E.; Zangrando, E.; Alessio, E. *Eur. J. Inorg. Chem.* **2003**, 2371–2384. (e) Alessio, E.; Iengo, E.; Marzilli, L. *Supramol. Chem.* **2002**, *14*, 103–120. (f) Baldini, L.; Hunter, C. A. *Adv. Inorg. Chem.* **2002**, *53*, 213–259.
- (5) Chang, C. J.; Brown, J. D. K.; Chang, M. C. Y.; Baker, E. A.; Nocera, D. G. In *Electron Transfer in Chemistry*; Balzani, V., Ed.; Wiley-VCH: Weinheim, Germany, 2001; Volume III, Part 2, Chapter 4, pp 409–461.
- (6) Drain, C. M.; Lehn, J.-M. *J. Chem. Soc., Chem. Commun.* **1994**, 2313–2315. (b) Yuan, H.; Thomas, L.; Woo, L. K. *Inorg. Chem.* **1996**, *35*, 2808–2817. (c) Slone, R. V.; Hupp, J. T. *Inorg. Chem.* **1997**, *36*, 5422–5423. (d) Stang, P. J.; Fan, J.; Olenyuk, B. *Chem. Commun.* **1997**, 1453–1454. (e) Drain, C. M.; Nifatis, F.; Vasenko, A.; Batteas, J. D. *Angew. Chem., Int. Ed.* **1998**, *37*, 2344–2347. (f) Fan, J.; Whiteford, J. A.; Olenyuk, B.; Levin, M. D.; Stang, P. J.; Fleischer, E. B. *J. Am. Chem. Soc.* **1999**, *121*, 2741–2752. (g) Fujita, N.; Biradha, K.; Fujita, M.; Sakamoto, S.; Yamaguchi, K. *Angew. Chem., Int. Ed.* **2001**, *40*, 1718–1721. (h) Iengo, E.; Milani, B.; Zangrando, E.; Geremia, S.; Alessio, E. *Angew. Chem., Int. Ed.* **2000**, *39*, 1096–1099. (i) Prodi, A.; Indelli, M. T.; Kleverlaan, C. J.; Alessio, E.; Scandola, F. *Coord. Chem. Rev.* **2002**, *229*, 48–55. (j) Iengo, E.; Zangrando, E.; Geremia, S.; Graff, R.; Kieffer, B.; Alessio, E. *Chem.–Eur. J.* **2002**, *8*, 4670–4674.
- (7) Fleischer, E. B.; Shachter, A. M. *Inorg. Chem.* **1991**, *30*, 3763–3769. (b) Chi, X.; Guerin, A. J.; Haycock, R. A.; Hunter, C. A.; Sarson, L. D. *J. Chem. Soc., Chem. Commun.* **1995**, 2567–2569. (c) Hunter, C. A.; Hyde, R. K. *Angew. Chem., Int. Ed. Engl.* **1996**, *35*, 1936–1939. (d) Würthner, F.; Sautter, A.; Thalacker, C. *Angew. Chem., Int. Ed.* **2000**, *39*, 1243–1245. (e) Ercolani, G.; Ioel, M.; Monti, D. *New J. Chem.* **2001**, *25*, 783–789. (f) Hunter, C. A.; Tregoning, R. *Tetrahedron* **2002**, *58*, 691–697. (g) Balaban, T. S.; Goddard, R.; Linke-Schaetzl, M.; Lehn, J.-M. *J. Am. Chem. Soc.* **2003**, *125*, 4233–4239. (h) You, C.-C.; Würthner, F. *Org. Lett.* **2004**, *6*, 2401–2404.
- (8) Würthner, F.; You, C.-C.; Saha-Möller, C. R. *Chem. Soc. Rev.* **2004**, *33*, 133–146. (b) Iengo, E.; Zangrando, E.; Minatel, R.; Alessio, E. *J. Am. Chem. Soc.* **2002**, *124*, 1003–1013.

- (9) Funatsu, K.; Kimura, A.; Imamura, T.; Ichimura, A.; Sasaki, Y. *Inorg. Chem.* **1997**, *36*, 1625–1635. (b) Funatsu, K.; Kimura, A.; Imamura, T.; Ichimura, A.; Sasaki, Y. *Inorg. Chem.* **1998**, *37*, 1798–1804. (c) Alessio, E.; Geremia, S.; Mestroni, S.; Iengo, E.; Srnova, I.; Slouf, M. *Inorg. Chem.* **1999**, *38*, 869–875. (d) Alessio, E.; Geremia, S.; Mestroni, S.; Srnova, I.; Slouf, M.; Gianferrara, T.; Prodi, A. *Inorg. Chem.* **1999**, *38*, 2527–2529.
- (10) Endo, A.; Okamoto, Y.; Suzuki, K.; Shimamura, J.; Shimizu, K.; Satō, G. *P. Chem. Lett.* **1994**, 1317–1320. (b) Chichak, K.; Branda, N. R. *Chem. Commun.* **1999**, 523–524. (c) Chichak, K.; Walsh, M. C.; Branda, N. R. *Chem. Commun.* **2000**, 847–848. (d) Chichak, K.; Branda, N. R. *Chem. Commun.* **2000**, 1211–1212. (e) Campbell, K.; McDonald, R.; Branda, N. R.; Tykwinski, R. R. *Org. Lett.* **2001**, *3*, 1045–1048. (f) Gunter, M. J.; Bampos, N.; Johnstone, K. D.; Sanders, K. M. *New J. Chem.* **2001**, *25*, 166–173. (g) Iengo, E.; Zangrando, E.; Mestroni, S.; Fronzoni, G.; Stener, M.; Alessio, E. *J. Chem. Soc., Dalton Trans.* **2001**, 1338–1346.
- (11) Alessio, E.; Macchi, M.; Heath, S.; Marzilli, L. G. *Chem. Commun.* **1996**, 1411–1412. (b) Prodi, A.; Indelli, M. T.; Kleverlaan, C. J.; Scandola, F.; Alessio, E.; Gianferrara, T.; Marzilli, L. G. *Chem.–Eur. J.* **1999**, *5*, 2668–2679.
- (12) Prodi, A.; Chiorboli, C.; Scandola, F.; Iengo, E.; Alessio, E. Manuscript in preparation.

Chart 2

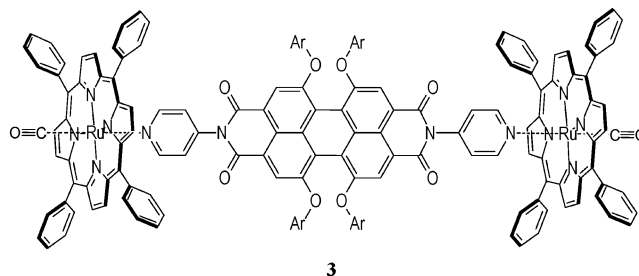


DPYPBI

With regard to metallosupramolecular coordination chemistry, PBI derivatives carrying 4-pyridyl substituents at the imido positions are of particular interest. An example is the DPYPBI molecule shown in Chart 2 (in which additional *tert*-butylphenoxy substituents have been introduced in the bay region to improve solubility and minimize aggregation phenomena).¹⁶ In molecules of this type, given the presence of nodes at the imido nitrogens in the HOMO and LUMO of the PBI unit,^{13g} the pyridyl substituents are effectively decoupled from the chromophore. This is an important feature when coordination of the pyridyl groups at metal centers is considered, as it ensures weak metal–chromophore electronic coupling and a true supramolecular nature of the adducts. The pyridyl-substituted perylene bisimide dyes can be used in the construction of supramolecular systems much in the same way as other ditopic building blocks. For instance, DPYPBI forms metal-bridged molecular squares with platinum or palladium biphosphine corners¹⁶ structurally similar to those given by *trans*-dipyridylporphyrins.^{6f} Following this functional analogy, it is conceivable that axial coordination of DPYPBI to metal porphyrins may lead to supramolecular systems structurally similar to side-to-face porphyrin arrays such as **1** and **2**.

We report here on the synthesis and photophysical properties of the first system of such type,¹⁷ the DPYPBI[Ru(TPP)(CO)]₂ assembly **3** (TPP = tetraphenylporphyrin), obtained by axial coordination of a DPYPBI unit to two Ru(TPP)(CO) fragments.

The structural analogy between **3** and side-to-face porphyrin arrays **1** and **2** is evident, with the DPYPBI unit replacing the



3

pyridylporphyrin in the role of the “side” assembling unit. On the other hand, the distinctive properties of the DPYPBI unit (especially in terms of low-energy redox levels) are expected to give to DPYPBI[Ru(TPP)(CO)]₂ a richer and more intriguing photophysical behavior as compared to that of the analogous side-to-face porphyrin array **1**.

Experimental Section

Materials. [Ru(TPP)(CO)(EtOH)] was prepared according to literature methods.¹⁸ DPYPBI was synthesized as previously reported.¹⁶ All reagents were analytical grade.

DPYPBI[Ru(TPP)(CO)]₂ (3). Addition of DPYPBI (10 mg, 8.8 × 10⁻⁴ mmol) to a chloroform suspension of [Ru(TPP)(CO)(EtOH)] (14.2 mg, 1.77 × 10⁻³ mmol) yielded a violet solution within minutes. The system was allowed to react overnight at room temperature. The crude product precipitated from the concentrated solution upon addition of *n*-hexane and was collected on a filter, washed with cold methanol and *n*-hexane, and vacuum-dried, with a yield of 21 mg (90%). The product gave satisfactory elemental analysis. ¹H NMR (CDCl₃, 400 MHz, 25 °C): δ βH 8.56 (16, s), mH 8.16 (8, m), oH 8.03 (8, m), H_b + oH' + pH 7.67 (20, m), mH 7.60 (8, m), H_e 7.03 (8, d), H_d 6.51 (8, d), H_c 5.12 (4, d), H_a 1.60 (4, d), *t*Bu 1.17 (36, s) (see Figure 1 for labeling scheme).

Apparatus. ¹H and H–H COSY NMR spectra were collected in CDCl₃ at room temperature and at 400 MHz on a JEOL Eclipse 400 FT spectrometer, with residual nondeuterated solvent signal as reference (δ = 7.26). UV–vis absorption spectra were recorded with a Perkin-Elmer Lambda 40 spectrophotometer. Nanosecond emission lifetimes were measured using a PRA system 3000 time-correlated single photon counting apparatus equipped with a Norland model 5000 MCA card and a hydrogen discharge pulsing lamp (50 kHz, halfwidth of 2 ns). The decays were analyzed by means of Edinburgh FLA900 software.

Nanosecond transient absorption spectra and lifetimes were measured with an Applied Photophysics laser flash photolysis apparatus, with frequency doubled (532 nm, 330 mJ) or tripled (355 nm, 160 mJ) Surelite Continuum II Nd:YAG laser (halfwidth of 4–6 ns). Photomultiplier (Hamamatsu R928) signals were processed by means of a LeCroy 9360 (600 MHz, 5 Gs/s) digital oscilloscope.

Femtosecond time-resolved experiments were performed using a pump–probe spectrometer¹⁹ based on the Spectra-Physics Hurricane Ti:sapphire system as laser source. The pump pulse was generated either by a frequency doubler (400 nm) or with a Spectra Physics 800 OPA (tunable in the 488–600 nm range). The probe pulse was obtained by continuum generation on a sapphire plate (useful spectral range, 450–800 nm). The effective time resolution was ca. 300 fs, the temporal chirp over the white-light 450–750 nm range was ca. 200 fs, and the temporal window of the optical delay stage was 0–1000 ps.

Results and Discussion

Synthesis and Characterization of DPYPBI[Ru(TPP)(CO)]₂. Addition of DPYPBI to a chloroform suspension of

- (13) Würthner, F.; Thalacker, C.; Sautter, A. *Adv. Mater.* **1999**, *11*, 754–758. (b) Würthner, F.; Thalacker, C.; Sautter, A.; Schärtl, W.; Ibach, W.; Hollricher, O. *Chem.–Eur. J.* **2000**, *6*, 3871–3888. (c) Schenning, A. P. H. J.; v. Herrikhuysen, J.; Jonkheijm, P.; Chen, Z.; Würthner, F.; Meijer, E. W. *J. Am. Chem. Soc.* **2002**, *124*, 10252–10253. (d) You, C.-C.; Würthner, F. *J. Am. Chem. Soc.* **2003**, *125*, 9716–9725. (e) Würthner, F.; Sautter, A. *Org. Biomol. Chem.* **2003**, *1*, 240–243. (f) Miura, A.; Chen, Z.; Uji-i, H.; De Feyter, S.; Zdanowska, M.; Jonkheijm, P.; Schenning, A. P. H. J.; Meijer, E. W.; Würthner, F.; De Schryver, F. C. *J. Am. Chem. Soc.* **2003**, *125*, 14968–14969. (g) Würthner, F. *Chem. Commun.* **2004**, 1564–1579.
- (14) Salbeck, J.; Kunkely, H.; Langhals, H.; Saalfrank, R. W.; Daub, J. *Chimia* **1989**, *43*, 6–9.
- (15) O'Neil, M. P.; Gaines, G. L., III; Niemczyk, M. P.; Svec, W. A.; Gosztola, D.; Wasielewski, M. R. *Science* **1992**, *257*, 63–65. (b) Hayes, T.; Wasielewski, M. R.; Gosztola, D. *J. Am. Chem. Soc.* **2000**, *122*, 5563–5567. (c) van der Boom, T.; Hayes, R. T.; Zhao, Y.; Bushard, P. J.; Weiss, E. A.; Wasielewski, M. R. *J. Am. Chem. Soc.* **2002**, *124*, 9582–9590. (d) Weiss, E. A.; Ahrens, M. J.; Sinks, L. E.; Gusev, A. V.; Ratner, M. A.; Wasielewski, M. R. *J. Am. Chem. Soc.* **2004**, *126*, 5577–5584. (e) Ahrens, M. J.; Sinks, L. E.; Rytchinski, B.; Liu, W.; Jones, B. A.; Giaimo, J. M.; Gusev, A. V.; Goshe, A. J.; Tiede, D. M.; Wasielewski, M. R. *J. Am. Chem. Soc.* **2004**, *126*, 8284–8294. (f) Giaimo, J. M.; Gusev, A. V.; Wasielewski, M. R. *J. Am. Chem. Soc.* **2004**, *126*, 8530–8531. (g) Kaletas, B. K.; Dobrawa, R.; Sautter, A.; Würthner, F.; Zimine, M.; De Cola, L.; Williams, R. M. *J. Phys. Chem. A* **2004**, *108*, 1900–1909.
- (16) Würthner, F.; Sautter, A.; Schmid, D.; Weber, P. *J. Am. Chem.–Eur. J.* **2001**, *7*, 894–902.
- (17) A few supramolecular systems based on axial coordination of other aromatic bisimides to metal porphyrins have recently been reported: (a) Flamigni, L.; Johnson, M. R.; Giriababu, L. *Chem.–Eur. J.* **2002**, *8*, 3938–3947. (b) Otsuki, J.; Suka, A.; Yamazaki, K.; Abe, H.; Araki, Y.; Ito, O. *Chem. Commun.* **2004**, 1290–1291.

- (18) Bonnet, J. J.; Eaton, S. S.; Eaton, G. R.; Holm, R. H.; Ibers, J. A. *J. Am. Chem. Soc.* **1973**, *95*, 2141–2149. (b) Collman, J. P.; Barnes, C. E.; Brothers, P. J.; Collins, T. J.; Ozawa, T.; Gallucci, J. C.; Ibers, J. A. *J. Am. Chem. Soc.* **1984**, *106*, 3500–3510.
- (19) Chiorboli, C.; Rodgers, M. A. J.; Scandola, F. *J. Am. Chem. Soc.* **2003**, *125*, 483–491.

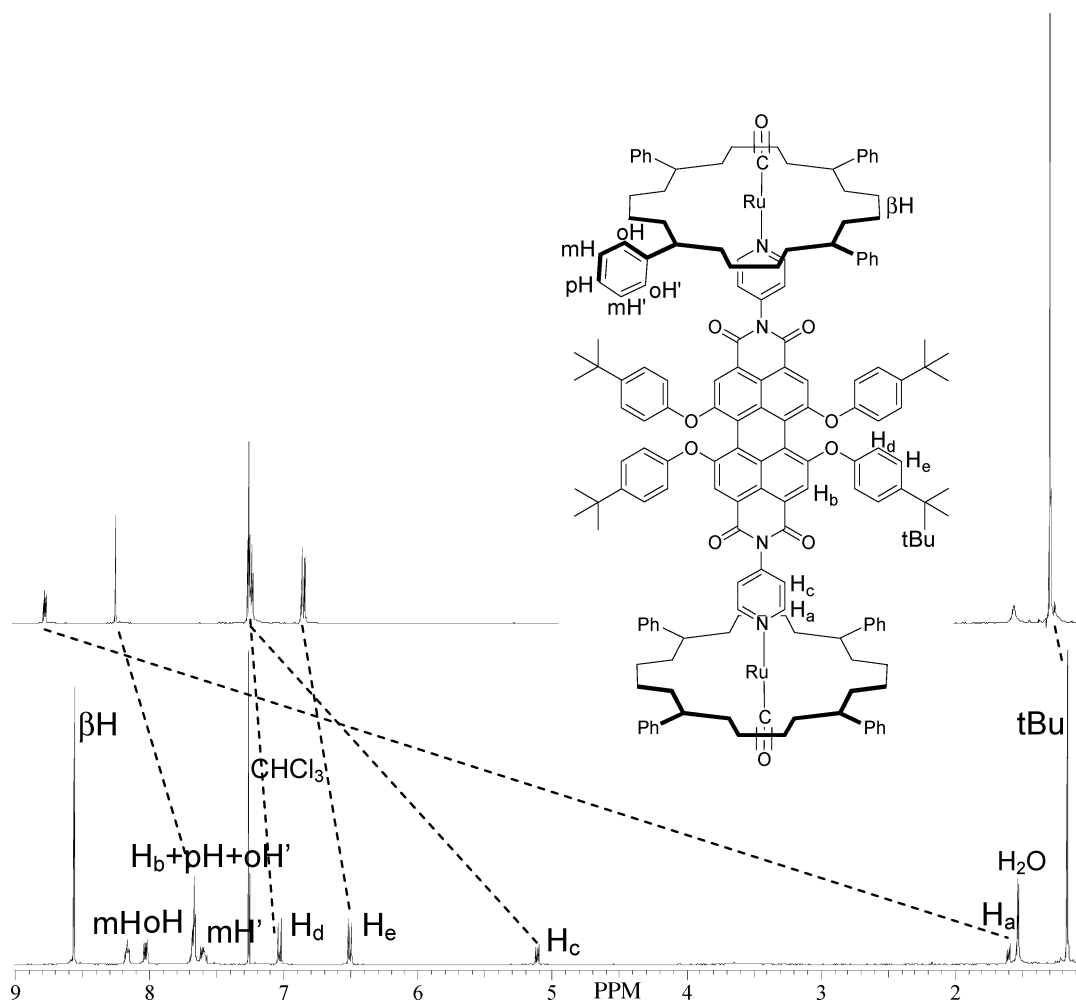


Figure 1. Comparison of the ^1H NMR (400 MHz, CDCl_3) of DPyPBI (top trace) and of DPyPBI[$\text{Ru}(\text{TPP})(\text{CO})_2$] (**3**) (bottom trace) with the difference in shift for DPyPBI induced by axial coordination to two $\text{Ru}(\text{TPP})(\text{CO})$ units indicated.

[$\text{Ru}(\text{TPP})(\text{CO})(\text{EtOH})$] led, within hours at room temperature, to the quantitative formation of DPyPBI[$\text{Ru}(\text{TPP})(\text{CO})_2$] (**3**), which was isolated in pure form as a deep violet powder. The product was characterized by means of NMR spectroscopy. Signal integration revealed the adduct stoichiometry, while an H–H COSY spectrum allowed unambiguous signal assignments. In the ^1H NMR of **3** in CDCl_3 , the resonances of the DPyPBI bridging unit shift remarkably upfield, as would be expected for protons that reside within the additive shielding cones of the facing porphyrins (Figure 1).^{7,9,11a} This effect decreases gradually as the proton distance from the shielding macrocycles increases, with the pyridyl protons being the most affected ones ($\Delta\delta = -7.18$ and $\Delta\delta = -2.14$ for H_a and H_c , respectively; see Figure 1). In addition, although all eight porphyrin phenyl rings are equivalent, the pairs of ortho and meta protons of each ring are nonequivalent due to slow rotation about the *meso*-carbon to the phenyl carbon bond, evidencing the different magnetic environment of the two sides of the porphyrin plane.²⁰ The most upfield shifted resonances of each pair have been assigned to the *endo*-phenyl protons, oH' and mH' (Figure 1).

A titration of DPyPBI with [$\text{Ru}(\text{TPP})(\text{CO})(\text{EtOH})$] has been followed by ^1H NMR in CDCl_3 . Coordination to the metal-

lorporphyrin is strong, and ligand exchange is slow on the NMR time scale. Sharp, unchanging peaks for the statistical mixture of mono- and diaddition products were clearly visible when less than 2 molar equiv of [$\text{Ru}(\text{TPP})(\text{CO})(\text{EtOH})$] was added. This observation could be particularly useful for further developments, such as assembling of three-component photoactive systems.

Properties of Molecular Components. The DPyPBI component is available as a free molecular species. A good model for the ruthenium porphyrin component is the $\text{Ru}(\text{TPP})(\text{CO})(\text{py})$ molecule.²¹ The photophysical behavior of the two models can be summarized as follows.

DPyPBI. The absorption spectrum is shown in Figure 2. The fluorescence of DPyPBI ($\lambda_{\text{max}} = 618$ nm in CH_2Cl_2) has a quantum yield of almost unity ($\Phi = 0.96$ in CHCl_3).¹⁶ The lifetime of the S_1 state is 7.2 ns in CH_2Cl_2 , as measured by single-photon counting techniques. Its differential absorption spectrum (Figure 3) shows ground-state bleaching at $\lambda < 600$ nm, some apparent bleaching due to stimulated emission at $600 < \lambda < 675$ nm, and excited-state absorption at $\lambda > 675$ nm. Consistent with the high fluorescence quantum yield, the

(20) Eaton, S. S.; Eaton, G. R.; Holm, R. H. *J. Organomet. Chem.* **1972**, *39*, 179–195. (b) Eaton, S. S.; Eaton, G. R. *J. Am. Chem. Soc.* **1975**, *97*, 3660–3666.

(21) Brown, G. M.; Hopf, F. R.; Ferguson, J. A.; Meyer, T. J.; Whitten, D. G. *J. Am. Chem. Soc.* **1973**, *95*, 5939–5942.

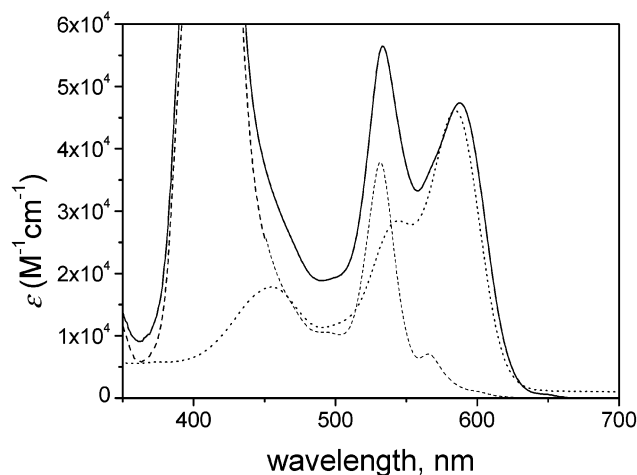


Figure 2. Absorption spectra of DPyPBI[Ru(TPP)(CO)]₂ (continuous line), DPyPBI (dotted line), and Ru(TPP)(CO)(py) (broken line, molar absorptivity values $\times 2$) in CH₂Cl₂.

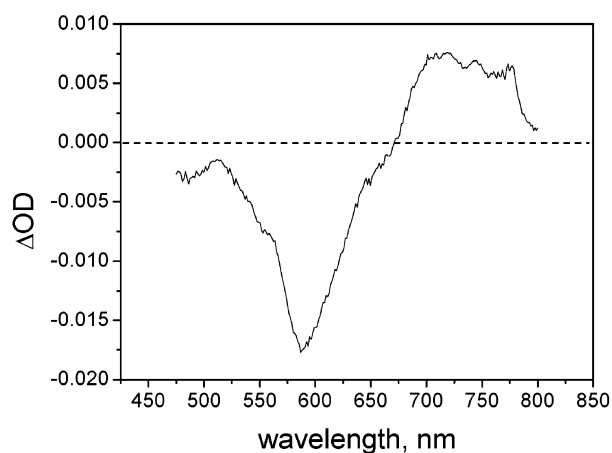


Figure 3. Transient differential absorption spectrum of DPyPBI in CH₂Cl₂ (excitation at 400 nm). Constant in the 1–1000 ps time scale.

population of triplet state by intersystem crossing is negligible.²² As a consequence, no transient absorption is observed in laser flash photolysis of DPyPBI after 10 ns. Information on the triplet state of the parent perylene bisimide dyes (i.e., those without substituents in the bay area) has been obtained by the use of bimolecular sensitization techniques (absorption maximum at ca. 500 nm, lifetime in the 10¹–10² μs range, estimated energy of ca. 1.2 eV).²³ The energy level diagram and photophysical behavior of DPyPBI are summarized in Figure 4a.

In CH₂Cl₂, DPyPBI undergoes two reversible electrochemical reduction steps at –0.62 and –0.77 V versus SCE (in addition to an irreversible oxidation process at ca. +1.6 V).^{16,24,25} As shown by spectroelectrochemistry, the one- and two-electron-reduced forms are characterized by intense, sharp absorption bands at 792 and 678 nm, respectively.¹⁶

Ru(TPP)(CO)(py). The absorption spectrum is shown in Figure 2. No fluorescence emission is observed from this

molecule as a consequence of the strong spin–orbit coupling provided by the heavy metal, leading to very fast S₁ → T₁ intersystem crossing.²⁶ A weak phosphorescence emission ($\Phi \approx 1 \times 10^{-3}$, $\lambda_{\text{max}} = 726$ nm) is observed in deaerated fluid solution.¹¹ The triplet state can be conveniently monitored at room temperature by transient absorption spectroscopy. The differential absorption spectrum obtained with ultrafast spectroscopy is shown in Figure 5. It is formed in less than 1 ps and is constant in the 1–1000 ps time window. In laser flash photolysis, it is observed to decay with $\tau = 30$ μs.¹¹ The photophysical behavior of the Ru(TPP)(CO)(py) model compound is summarized in Figure 4b.

In CH₂Cl₂, Ru(TPP)(CO)(py) undergoes two reversible electrochemical oxidation steps at 0.81 and 1.36 V versus SSCE.²¹

Photophysics of the DPyPBI[Ru(TPP)(CO)]₂ Assembly.

Stability in Solution. Similar to that for previously studied side-to-face arrays of type **1**, stability in (dilute) solution is a key experimental question related to the moderate strength of the coordinative bond between the pyridyl group of the side unit and the metal center of the face porphyrin. The stability of DPyPBI[Ru(TPP)(CO)]₂ in CH₂Cl₂ solutions was checked by a combination of NMR, spectrophotometric, and spectrofluorimetric measurements. The absorption spectrum of DPyPBI[Ru(TPP)(CO)]₂, at a concentration of 1.0 $\times 10^{-4}$ M, corresponding to the maximum dilution at which stability of the assembly is assessed by NMR, is shown in Figure 2. No appreciable spectral changes indicative of dissociation are obtained upon further dilution to 2.0 $\times 10^{-5}$ M.²⁷ Also, the strong quenching of the DPyPBI fluorescence characteristic of the assembly (vide infra) was maintained to this dilution. At higher dilutions ($\leq 1.0 \times 10^{-5}$ M), some axial dissociation takes place, as shown mainly by a slight increase in the DPyPBI fluorescence intensity. All of the photophysical experiments described below were carried out in CH₂Cl₂ at concentrations greater than 2.0 $\times 10^{-5}$ M.

Energy Levels. As shown by Figure 2, the absorption spectrum of DPyPBI[Ru(TPP)(CO)]₂ (**3**) corresponds very closely to the sum of those of its molecular components. This highlights the supramolecular nature of the assembly, in which the weakly interacting molecular components maintain almost unperturbed electronic subsystems. In practical terms, this feature implies that selective excitation is feasible (e.g., 100% DPyPBI at 585 nm, 62% Ru(TPP)(CO) at 530 nm). From a mechanistic viewpoint, the energy level diagram of **3** can be considered as a simple superposition of those of the separated constituents. To such an energy level diagram, however, must be added an intercomponent charge transfer state of DPyPBI[–]/Ru(TPP)(CO)⁺-type (Figure 6). Its energy is estimated as ca. 1.3 eV from the electrochemistry of the single units (vide supra).^{28,29}

(26) Levine, L. M. A.; Holten, D. *J. Phys. Chem.* **1988**, *92*, 714–720.

(27) In previous studies on related systems, axial dissociation was indicated by blue shifts in the 531 nm band of the ruthenium porphyrin chromophore.¹¹

(28) In a covalently linked donor–acceptor system, both covalent and electrostatic factors may alter the energy of the charge-transfer state with respect to the simple algebraic sum of the redox potentials of the units. Given the weakly coupled nature of these supramolecular systems, covalent corrections are likely to be negligible in this case. The electrostatic work term can be taken into account using standard expressions.²⁹

(29) Rehm, D.; Weller, A. *Ber. Bunsen-Ges. Phys. Chem.* **1969**, *73*, 834–839. (b) Weller, A. *Z. Phys. Chem.* **1982**, *133*, 93. The electrostatic work term in CH₂Cl₂, at an estimated center-to-center distance of 12.5 Å, amounts to 0.13 eV.

(22) A very low value of triplet formation yield (1.8×10^{-4}) has recently been reported for a related chromophore: Margineanu, A.; Hofkens, J.; Cotlet, M.; Habuchi, S.; Stefan, A.; Qu, J.; Kohl, C.; Müllen, K.; Vercammen, J.; Engelborghs, Y.; Gensch, T.; De Schryver, F. C. *J. Phys. Chem. B* **2004**, *108*, 12242–12251.

(23) Ford, W. E.; Kamat, P. V. *J. Phys. Chem.* **1987**, *91*, 6373–6380.

(24) Original values versus Fc/Fc⁺,¹⁶ converted using $E^\circ(\text{Fc}/\text{Fc}^+) = 0.46$ V versus SCE.²⁵

(25) Connelly, N. G.; Geiger, W. E. *Chem. Rev.* **1996**, *96*, 877–910.

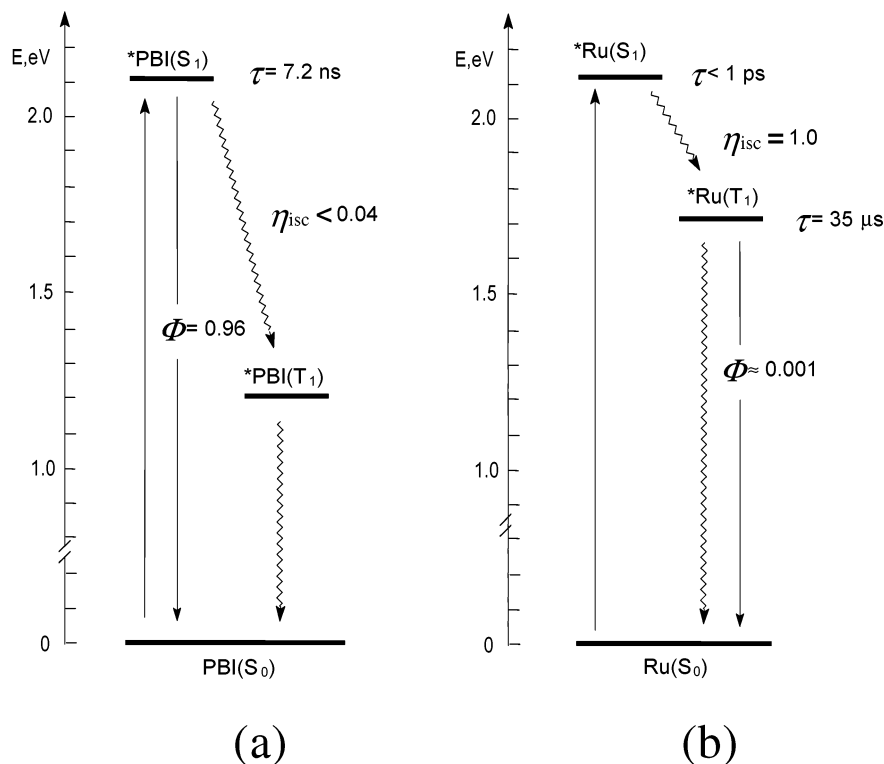


Figure 4. Energy level diagram and photophysical behavior of molecular components: (a) DPyPBI, (b) Ru(TPP)(CO)(py).

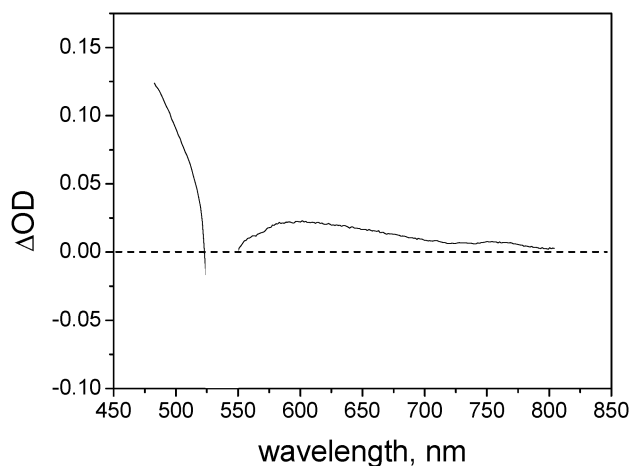


Figure 5. Transient differential absorption spectrum of Ru(TPP)(CO)(py) in CH₂Cl₂ (excitation at 530 nm). Constant in the 1–1000 ps time scale.

Excitation at 585 nm. At this wavelength, the excitation light is 100% absorbed by the DPyPBI component (Figure 2). In stationary experiments on **3** in CH₂Cl₂, the strong fluorescence ($\lambda_{\text{max}} = 620$ nm) characteristic of the DPyPBI unit is almost completely quenched ($\Phi \approx 0.001$, as compared to $\Phi = 0.96$ for free DPyPBI).

Three mechanisms could, in principle, be considered responsible for the strong quenching of the DPyPBI fluorescence.

(i) Intercomponent electron transfer to yield the PBI⁻/Ru⁺ charge-separated state. Very fast photoinduced electron transfer has been reported to occur in covalently linked arrays of PBI and Zn porphyrins of comparable energetics.^{15c}

(ii) Enhanced intersystem crossing within the DPyPBI unit induced by the heavy-atom effect of the attached ruthenium centers. Such intramolecular effects have been previously

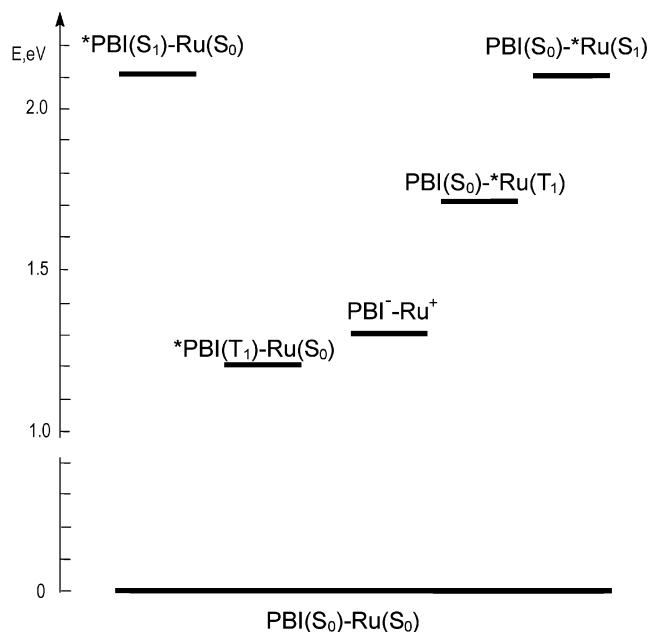


Figure 6. Energy level diagram of DPyPBI[Ru(TPP)(CO)]₂ (**3**).

observed for adducts of pyridylporphyrins peripherally coordinated to ruthenium centers.³⁰ An external heavy-atom effect has also been reported for a related perylene bisimide fluorophore in methyl iodide solvent.³¹

(iii) Intercomponent energy transfer to the almost isoenergetic S₁ state of the Ru(TPP)(CO) units.³²

An experimental answer is provided by ultrafast time-resolved spectroscopy.

(30) Prodi, A.; Kleverlaan, C. J.; Indelli, M. T.; Scandola, F.; Alessio, E.; Ingó, E. *Inorg. Chem.* **2001**, *40*, 3498–3504.

(31) Ebeid, E. M.; El-Daly, S. A.; Langhals, H. *J. Phys. Chem.* **1988**, *92*, 4565–4568.

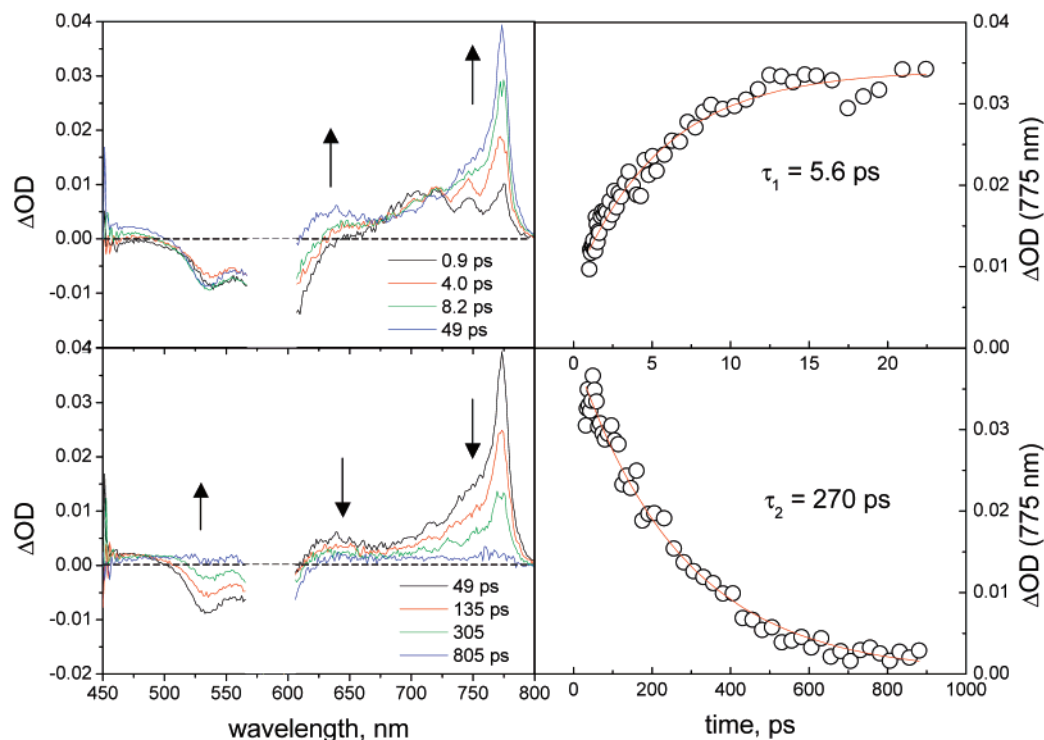


Figure 7. Transient spectral changes (left) and decay kinetics (right) of **3** in CH_2Cl_2 obtained with ultrafast spectroscopy upon excitation at 585 nm. Top, early time scale (0.9–48 ps); bottom, longer time scale (48–805 ps).

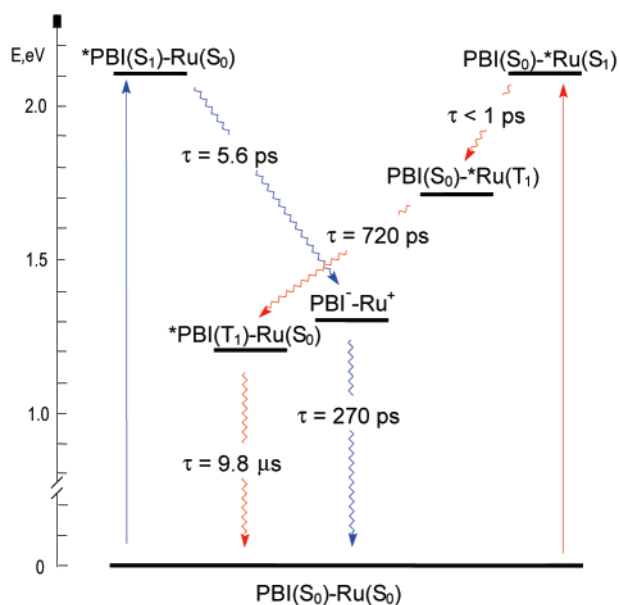


Figure 8. Photophysical pathways in $\text{DPyPBI}[\text{Ru}(\text{TPP})(\text{CO})]_2$ (**3**). Red, excitation at 530 nm; blue, excitation at 585 nm.

The transient spectral changes obtained following 585 nm excitation of **3** in CH_2Cl_2 are shown in Figure 7. As expected on the basis of the selective absorption of the pump light, the differential absorption spectrum obtained immediately after the laser pulse (0.9 ps) is that of the S_1 state of the DPYPBI unit, identical to that exhibited by free DPYPBI (Figure 3). In the early time scale ($\tau < 50$ ps, Figure 7, top left), the spectral changes are characterized by the rise of the typical absorption

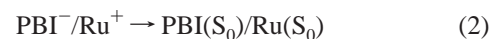
(32) It should be pointed out that while the energy of the S_1 state of the DPYPBI component is precisely known from absorption/emission data, that of the S_1 state of the $\text{Ru}(\text{TPP})(\text{CO})$ units, estimated from the onset of absorption, is affected by a considerable uncertainty (± 0.1 eV).

band of the DPYPBI radical anion at ca. 780 nm,¹⁶ with the $\text{Ru}(\text{TPP})(\text{CO})$ -based radical cation probably contributing to some positive absorption in the region around 630 nm.^{33,34} These spectral changes are clearly diagnostic of the electron-transfer process (eq 1).



The time constant of this process is 5.6 ps (Figure 7, top right).

On a longer time scale ($50 < \tau < 1000$ ps, Figure 7, bottom left), the spectroscopic signatures of the intercomponent electron-transfer products disappear, with regeneration of a constant baseline of zero differential absorption. This clearly indicates that the charge separation process (eq 1) is followed by charge recombination (eq 2) to yield quantitatively, after ca. 1 ns, the ground state of the system.³⁵



The time constant of this charge recombination process is 270 ps (Figure 7, bottom right).

(33) The spectrum of the radical cation of $\text{Ru}(\text{TPP})(\text{CO})(\text{py})$ is not known. Radical cations of other metalloporphyrins (e.g., zincporphyrin), however, are known to have broad visible absorption spectra with maxima in the 600–680 nm range.³⁴

(34) Fajer, J.; Borg, D. C.; Forman, A.; Dolphin, D.; Felton, R. H. *J. Am. Chem. Soc.* **1970**, *92*, 3451–3459. (b) Chosrowjan, H.; Taniguchi, S.; Okada, T.; Takagi, S.; Arai, T.; Tokumaru, K. *Chem. Phys. Lett.* **1995**, *242*, 644–649. (c) Imahori, H.; Hagiwara, K.; Aoki, M.; Akiyama, T.; Taniguchi, S.; Okada, T.; Shirakawa, M.; Sakata, Y. *J. Am. Chem. Soc.* **1996**, *118*, 11771–11782.

(35) It can be noted that no absorption maximum at 515 nm, characteristic of the DPYPBI triplet, is observed at the end of the experiment. Thus, in contrast with what has been observed for related supramolecular systems containing PBI and $\text{Zn}(\text{TPP})$ units,^{15c} no perylene bisimide triplet is formed here as a consequence of charge recombination. Charge recombination is probably too fast in the present case for intersystem crossing to occur within the charge-separated state.

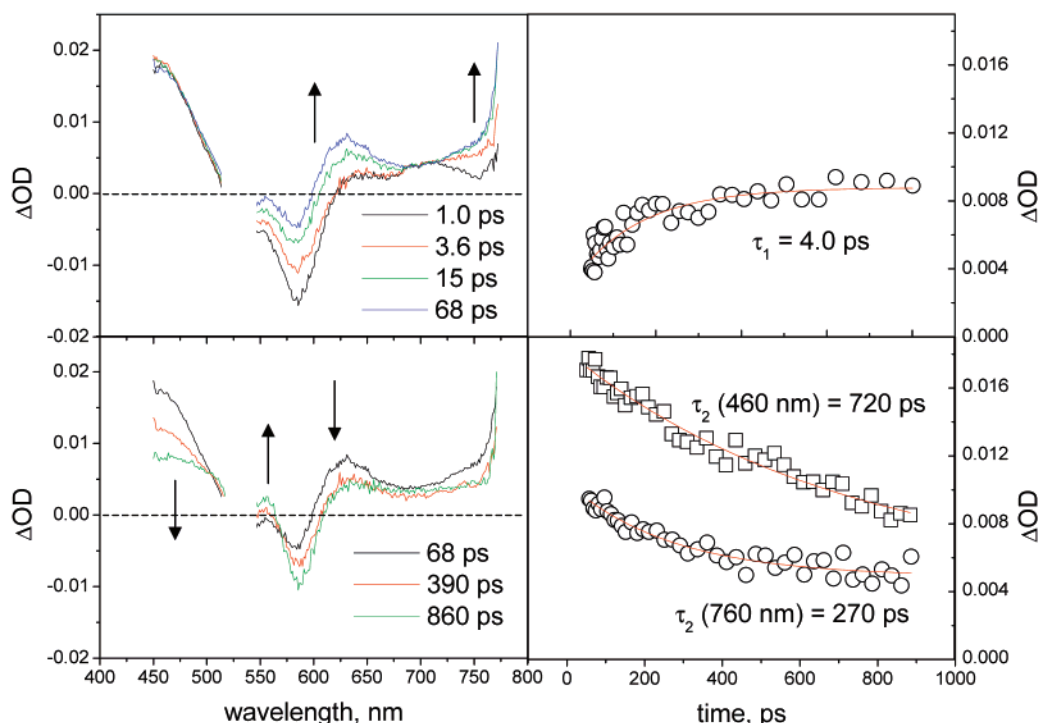


Figure 9. Transient spectral changes (left) and decay kinetics (right) obtained for **3** in CH_2Cl_2 with ultrafast spectroscopy upon excitation at 530 nm. Top, early time scale (1–68 ps); bottom, longer time scale (68–860 ps).

In conclusion, as depicted in Figure 8, the main pathway for deactivation of the singlet excited state of the DPyPBI unit in **3** is reductive electron transfer followed by charge recombination.

Excitation at 530 nm. At this wavelength, the excitation light is absorbed ca. 62% by $\text{Ru}(\text{TPP})(\text{CO})$ and 38% by DPyPBI. In stationary experiments, a very weak, strongly quenched DPyPBI fluorescence ($\lambda_{\text{max}} = 620 \text{ nm}$) is observed, as expected on the basis of the fraction of direct light absorption by this unit. On the other hand, no appreciable $\text{Ru}(\text{TPP})(\text{CO})$ phosphorescence ($\lambda_{\text{max}} = 726 \text{ nm}$) is observed.³⁶

Interestingly, the ultrafast spectroscopy obtained with 530 nm excitation differs dramatically from that observed with 585 nm excitation. The spectral variations are depicted in Figure 9.

The differential spectrum immediately after the laser pulse (1.0 ps) in Figure 9 shows a positive absorption with a maximum at 460 nm, diagnostic of the T_1 excited state of the $\text{Ru}(\text{TPP})(\text{CO})$ fragment (very similar to that exhibited by the $\text{Ru}(\text{TPP})(\text{CO})(\text{py})$ model, Figure 5). In addition, as expected, it shows features characteristic of the S_1 state of the perylene bisimide unit (mainly ground-state bleaching in the 550–600 nm region, and stimulated emission in the 600–675 nm range; see Figure 3). In the early time scale ($\tau < 68 \text{ ps}$, Figure 9, top), the 460 nm absorption remains constant, whereas in the 550–800 nm range, spectral changes practically coincident in shape and kinetics to those found for the 585 nm excitation (Figure 7, top) are observed. This indicates that the fraction of light (38%) absorbed by the DPyPBI unit gives rise, as expected, to fast electron transfer (eq 1), whereas the T_1 state generated by excitation of the $\text{Ru}(\text{TPP})(\text{CO})$ fragment does not decay appreciably in this time scale.

On a longer time scale (Figure 9, bottom), complex spectral changes take place. In particular, the DPyPBI radical anion absorption at 760 nm decays with the same kinetics as that observed for 585 nm excitation, indicating very likely the occurrence of charge recombination (eq 2). On the other hand, the absorption at $\lambda < 500 \text{ nm}$, characteristic of the $\text{Ru}(\text{TPP})(\text{CO})$ -based T_1 state, disappears with a time constant of 720 ps. It should be noted that this process is accompanied by a further bleaching at 580 nm, indicative of depletion of ground-state DPyPBI. The most likely explanation for this observation is the occurrence of triplet energy transfer (eq 3).



As the process is not completed within the time window of the ultrafast experiment, nanosecond laser photolysis can be used to obtain the spectrum of the product (i.e., the T_1 state of DPyPBI). The transient spectrum obtained with nanosecond laser photolysis upon excitation at 532 nm is shown in Figure 10. It shows spectral features (ground-state bleaching and absorption maximum at ca. 500 nm) similar to those reported for other perylene bisimide triplets, obtained by bimolecular sensitization with triplet energy donors.²³ The triplet state decays to the ground-state (eq 4) with a lifetime of 9.8 μs in deaerated CH_2Cl_2 (480 ns in air-saturated solution, Figure 10, inset).



The decay pathway followed after excitation of the $\text{Ru}(\text{TPP})(\text{CO})$ unit in **3** is summarized on the energy level diagram of Figure 8. After prompt intersystem crossing in the $\text{Ru}(\text{TPP})(\text{CO})$ unit, intercomponent triplet energy transfer takes place, followed by slow decay of the T_1 state of the DPyPBI unit. It should be noted that, in principle, an alternative pathway for

(36) An estimate of the actual amount of quenching is precluded by the intrinsic weakness ($\Phi \approx 1 \times 10^{-3}$) of the $\text{Ru}(\text{TPP})(\text{CO})$ phosphorescence, in the presence of a residual DPyPBI fluorescence of comparable intensity.

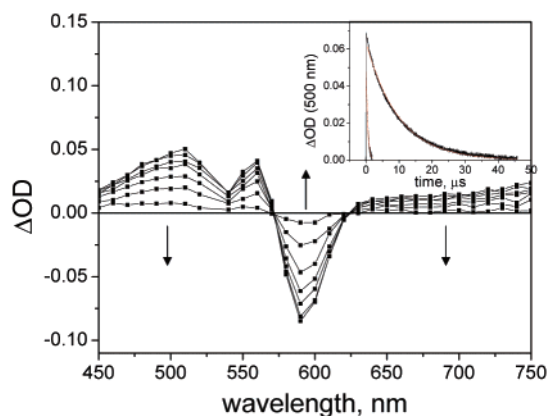


Figure 10. Transient spectral changes of **3** in CH_2Cl_2 obtained with nanosecond laser photolysis upon excitation at 532 nm. Inset: decay kinetics in aerated/deaerated solution.

the formation of the T_1 state of the DPyPBI unit might involve a sequence of oxidative electron transfer, with formation of a PBI^-/Ru^+ state of triplet multiplicity, followed by charge recombination. There is no positive evidence for such a stepwise path; no electron-transfer products are seen in the nanosecond experiment, and those observed in ultrafast spectroscopy after 530 nm excitation (Figure 9) are largely explained by the partial light excitation of the DPyPBI fragment. Nevertheless, the possibility of a stepwise path cannot be definitely ruled out, in particular, if charge recombination is a fast process.

Conclusions

A self-assembling strategy has been applied in this work to the construction of a side-to-face supramolecular array made

of a perylene bisimide and two ruthenium porphyrins. Such synthetic strategy warrants the formation of a single supramolecular species in very high yield. The new assembling motif may offer some advantages over commonly used covalent bridging, especially in terms of synthetic ease and versatility. With this strategy, a variety of metal-bridged and side-to-face systems containing porphyrins and aromatic bisimides can be conceived. The synthesis and characterization of such systems is the subject of ongoing work.

The DPyPBI[$\text{Ru}(\text{TPP})(\text{CO})_2$] assembly exhibits complex and very interesting photophysics. It provides a rather striking example of wavelength-dependent behavior, in that a relatively small change in excitation wavelength (from 585 to 530 nm) causes a sharp change in photophysical behavior (from intramolecular electron transfer to triplet energy transfer).

The triplet state of perylene bisimide chromophores is inaccessible in the free molecules due to high fluorescence quantum yields and negligible intersystem crossing efficiency. Axial ligation of DPyPBI to the $\text{Ru}(\text{TPP})(\text{CO})_2$ moieties can be seen as a way to access the triplet state with high efficiency by means of intramolecular sensitization.

Finally, the present work, with the detailed kinetic characterization of a complex mechanistic scheme (Figure 8), clearly illustrates the great potential of ultrafast spectroscopic techniques in the investigation of photoactive supramolecular systems.

Acknowledgment. Financial support from MIUR (PRIN 2003 and FIRB-RBNE019H9K projects) and from the donors of the Petroleum Research Fund, administered by the ACS (Grant ACS PRF# 38892-AC3), is gratefully acknowledged.

JA045379U